Construction of C_{60} Monolayer Based on Structural Relaxation on the Water Surface

Masami Yanagida, Atsushi Takahara, and Tisato Kajiyama*

Department of Materials Physics and Chemistry, Graduate School of Engineering, Kyushu University, 6-10-1 Hakozaki, Higashi-ku, Fukuoka 812-8581

(Received January 5, 2000)

A C_{60} monolayer was constructed by a multi-step creep method for the first time. In the case that a dilute C_{60} benzene solution of 1×10^{-5} M (1 M = 1 mol dm^{-3}) was spread on the water surface, C_{60} molecules formed into highly organized 2-dimensional crystalline domains. On the other hand, in the case of the conventional continuous compression method up to a low surface pressure below 15 mN m^{-1}, the C_{60} monolayer-like aggregates were formed with a lot of vacancies. Each monolayer-like C_{60} aggregate was easily collapsed into small fragments and changed into 3-dimensional aggregates at a high surface pressure above 20 mN m^{-1}. The C_{60} film could not full up the vacancies during continuous compression, since the C_{60} molecules formed rigid aggregates. These results clearly indicate that structural relaxation at a low surface pressure was required to construct the defect-diminished C_{60} monolayer. The occupied area of a C_{60} molecule in the monolayer prepared by the multi-step creep method was in good agreement with that of a 2-dimensional C_{60} crystal calculated from lattice constants of a 3-dimensional C_{60} crystal. The surface morphology of the C_{60} monolayer prepared by the multi-step creep method was homogeneous, and C_{60} molecules in the monolayer were closely and regularly packed in a hexagonal array. The hexagonal packing of the C_{60} molecules was confirmed on the basis of atomic force microscopic and electron diffraction observations.

Since the discovery of buckminsterfullerene (C_{60})[1] and of a efficient preparation method for large quantities of C_{60},[2] the C_{60} molecules have attracted much attention because of their characteristic structure and interesting physical properties such as superconductivity at a high temperature,[3—6] photoconductivity,[7] and high nonlinear optical coefficients.[8] In order to apply the C_{60} molecules as functional devices, one must construct the defect-free or defect-diminished C_{60} ultra-thin films. Langmuir–Blodgett (LB) technique may be the most useful method for construction of an ultra-thin film whose structure and film thickness are controlled at a molecular level.[9] The film of the intact C_{60} on the water surface has been investigated by several groups.[6,10—15] Since the C_{60} molecule without any chemical modification is not amphiphilic and exhibits strong intermolecular attractive force, however, the C_{60} molecules do not form the 2-dimensional C_{60} monolayer but easily aggregate into a 3-dimensional array instead of the formation of the C_{60} monolayer on the water surface.[12] Amphiphilic C_{60} molecules synthesized by chemical modification[14,16—20] or mixtures of C_{60} and fatty acid[12,21—23] were used to prepare the C_{60} monolayer on the water surface. However, since the existence of the modified parts on the C_{60} molecule or fatty acid may prevent the nature of C_{60} itself in the case of these monolayers, one must construct the C_{60} monolayer from the only C_{60} molecule without any chemical modification. Some groups have reported that in the case of using a very dilute solution of C_{60}, the C_{60} monolayer could be prepared on the water surface.[6,10] However, the aggregation structure of the C_{60} monolayer on the water surface was not investigated in detail.

The area–creep behavior of fatty acid monolayers has been studied to construct the defect-diminished fatty acid monolayer on the water surface.[24—26] The monolayer on the water surface generally exhibits area–creep phenomena, that is, a surface area decreases with an increase in a creep time at a constant surface pressure.[24—28] Since the area–creep behavior of the monolayer strongly reflects the aggregation state of fatty acid molecules, the analyses of the area–creep behavior of the fatty acid must give us some useful information to construct the highly regularized monolayer. For the stearic acid monolayer, the surface area decreased with an increase in the creep time due to structural relaxation or collapse of the monolayer.[24] Therefore, the multi-step creep method will be one of the effective preparation methods for the defect-diminished monolayers on the water surface.[25] It is reasonable to consider that, as the multi-step creep method is based on the structural relaxation phenomena in the monolayer, the multi-step creep method might be useful for the construction of the morphologically and crystallographically homogeneous C_{60} monolayer.

In this study, the preparation of C_{60} monolayer has been discussed from the viewpoint of the structural relaxation in the C_{60} film prepared from a very dilute solution. Then, the aggregation structure of the C_{60} film prepared by the multi-step creep method was investigated on the basis of the transmission electron microscopic (TEM) and the atomic force microscopic (AFM) observations.

Experimental

Film Preparation. C_{60} was purchased with a quality of 99.99 % (Matsubo Co., Japan) and used without further purification. Benzene of spectroscopic grade was used as a spreading solvent. Benzene solutions of C_{60} were prepared with concentrations of 1.0×10^{-5} and 1.0×10^{-4} mol L^{-1}. The subphase water was purified with Milli-QII system (Millipore Co., Ltd.). The subphase temperature, T_{sp} was maintained by circulating constant-temperature water around an aluminium support of a trough; the accuracy of T_{sp} was ±0.1 K. The π–A isotherms of the C_{60} film was independent of T_{sp} within the temperature range of 283 to 318 K. Hence, the T_{sp} was fixed at 293 K in this study. The dimensions of the trough were 400 mm in length, 150 mm in width, and 5 mm in depth. A subphase water level was maintained by a home-made water level maintainer to prevent the decrease of the apparent surface pressure due to the evaporation of the subphase water.[25,26] The surface pressure was measured by the Wilhelmy balance technique. Compression and area–creep measurements of the monolayer were carried out with a microprocessor-controlled film balance system (USI System Co., Ltd., FSD-20). The C_{60} films were prepared by spreading 72 μL (for 1.0×10^{-4} mol L^{-1} solution) or 720 μL (for 1.0×10^{-5} mol L^{-1} solution) of the benzene solution of C_{60} on the water surface, and then compressed at the constant rate of 120 $mm^2\ s^{-1}$.

The defect-diminished C_{60} film was prepared by the multi-step creep method.[29] The C_{60} film was compressed up to the surface pressure of 15 mN m^{-1} at the constant rate of 120 $mm^2\ s^{-1}$, and then maintained at this surface pressure. In this process, the variation of the C_{60} film area was monitored to evaluate a quasi-equilibrium state in terms of the creep behavior. Then, the film was further compressed to 17 mN m^{-1} and again, maintained at 17 mN m^{-1}. By the technique of step-wise compression mentioned above, the C_{60} film was finally compressed to the surface pressure of 20 mN m^{-1}. Finally, the C_{60} film was transferred onto the solid substrate by the horizontal drawing-up method.[30]

Transmission Electron Microscopic Observation. The C_{60} films on the water surface were transferred onto a collodion substrate by the horizontal drawing-up method for TEM observation. The collodion substrate was prepared by a cover of the collodion thin film onto a glass slide on which electron microscope grids (200 mesh) were placed. It was confirmed from AFM (Seiko Instruments Inc., SPA300) observation and electron diffraction (ED) measurement that the surface of the collodion substrate was smooth enough to use and was in an amorphous state at 293 K. The ED patterns of the C_{60} films were obtained with TEM (Hitachi, H-7000), which was operated at an acceleration voltage of 75 kV and a beam current of a several μA. The electron beam was 10 μm in diameter. TEM observation was carried out at 293 K corresponding to T_{sp}. A lateral crystallographical regularity, that is, the magnitudes of crystallographical distortion (D_{lat}) and continuity (L_{lat}), of the 2-dimensional monolayers were evaluated by the single line method based on the Fourier analysis of the ED profiles.[31]

Atomic Force Microscopic Observation. The C_{60} films were transferred onto a freshly cleaved mica (Okabe Mica Co., Japan) substrate by the horizontal drawing-up method. AFM equipped with 20 μm scanner and a Si_3N_4 tip on a cantilever with the spring constant of 0.02 N m^{-1} was employed for the observation of the surface morphology of the C_{60} films. Also, a 1 μm scanner was used for the high-resolution observation of the C_{60} films. AFM images were recorded in the "constant force" mode for the observation on μm scale and the "constant height" mode for the high-resolution

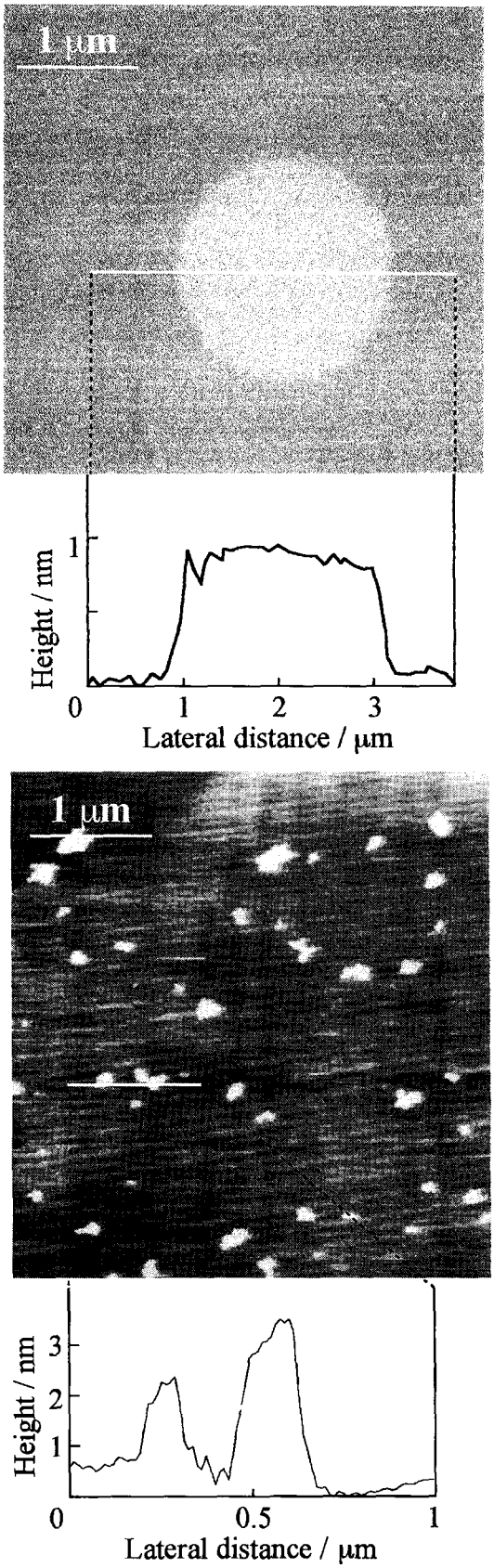

Fig. 1. AFM images of the C_{60} film prepared from the solution of 1.0×10^{-5} (a) and 1.0×10^{-4} mol L^{-1} (b) right after spreading solution and each height profiles along the straight line shown into Figs. 1(a) and 1(b), respectively.

observation on nm scale. AFM observation was carried out in air and at 293 K, the temperature at which the C_{60} films were prepared. The applied force for scanning was in a weak repulsive force range of ca. 10^{-10} N. Under this condition, the morphology of the C_{60} films could be obtained without any destruction by scanning the cantilever tip.

Results and Discussion

Possible Formation Mechanism of C_{60} Film during Continuous Compression. Figures 1(a) and 1(b) show the typical AFM images of the C_{60} films prepared from a solution of 1.0×10^{-5} (a) and of 1.0×10^{-4} mol L^{-1} (b), right after spreading the solution ($\pi = 0$ mN m^{-1}); their height profiles along the straight lines drawn in these Figures are displayed as well. In the case of the dilute solution of 1.0×10^{-5} mol L^{-1}, large isolated circular domains with 0.1 to several μm in diameter were observed. The average height of such an isolated circular C_{60} domain was ca. 0.9 nm, corresponding to the diameter of the C_{60} molecule including the π electron cloud.[32] On the other hand, in the case of the concentrated solution of 1.0×10^{-4} mol L^{-1}, the C_{60} molecules formed the smaller domains with irregular shapes and various heights of several nm, as shown in Fig. 1(b). Hence, Figs. 1(a) and 1(b) clearly indicate that the C_{60} molecules spontaneously formed the 2-dimensional domains right after spreading the dilute C_{60} solution ($< 1.0\times10^{-5}$ mol L^{-1}) on the water surface and also, the C_{60} molecules formed the 3-dimensional aggregates due to their strong intermolecular interaction in the case of the concentrated C_{60} solution ($> 1.0\times10^{-4}$ mol L^{-1}). This higher order molecular aggregation might arise from the fact that several C_{60} molecules were already associated together in the concentrated solution before spreading on the water surface. Therefore, it seems reasonable to conclude that the C_{60} monolayer can be formed on the water subphase when the dilute solution below 1.0×10^{-5} mol L^{-1} is used.

Figures 2(a) and 2(b) show the ED patterns of the C_{60} film prepared from the C_{60} benzene solution of 1.0×10^{-5} mol L^{-1} by the continuous compression method at the surface pressure of 0 (a) and 20 mN m^{-1} (b), respectively. The ED pattern of the C_{60} film prepared at 0 mN m^{-1} showed the hexagonal spots corresponding to the 2-dimensional crystalline hexagonal system. Therefore, Fig. 2(a) clearly indicates that the C_{60} molecules spontaneously formed the 2-dimensional crystalline domains on the water subphase right after spreading the dilute C_{60} benzene solution, as shown in Fig. 1(a). On the contrary, the ED pattern of the C_{60} film prepared by the continuous compression up to 20 mN m^{-1} was the crystalline Debye ring, as shown in Fig. 2(b). It can be considered from Fig. 2(b) that the C_{60} film was collapsed into small fragments during a continuous compression to a high surface pressure of about 20 mN m^{-1}, probably due to the rigidity of the C_{60} film.

Figure 3 shows the π–A isotherm of the C_{60} film prepared from the solution of 1.0×10^{-5} mol L^{-1} at 293 K. The limiting area evaluated from the π–A isotherm of the C_{60} film was 1.3 nm^2 $molecule^{-1}$. In contrast, the molecular occupied area in the 2-dimensional C_{60} hexagonal crystal

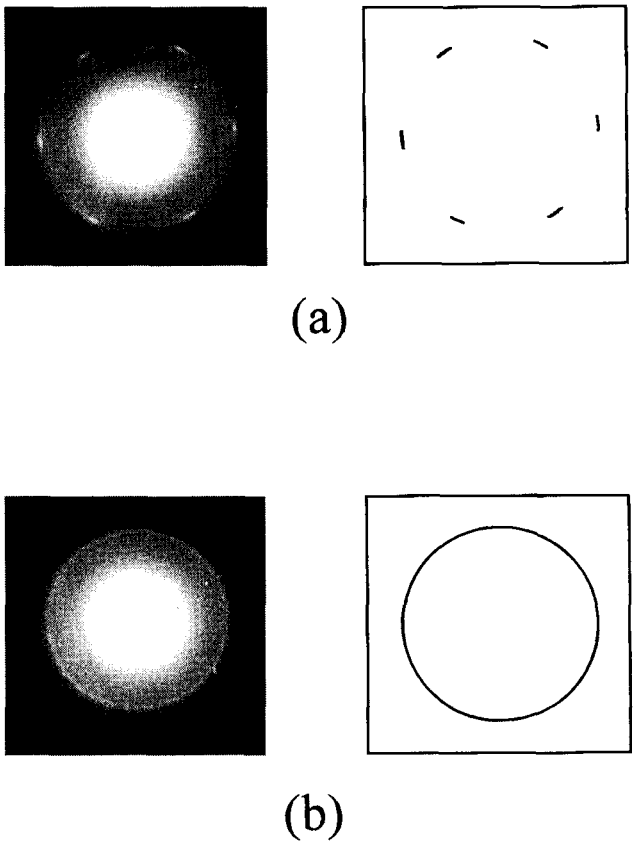

Fig. 2. Electron diffraction (ED) patterns of the C_{60} film prepared by the continuous compression method at the surface pressure of 0 (a) and 20 mN m^{-1} (b). Lefthand patterns were original, and righthand patterns were schematic diffraction on the same position to original diffraction.

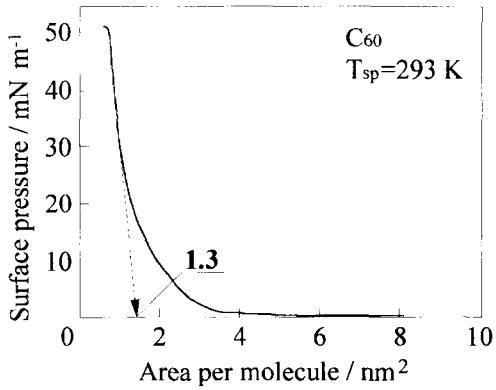

Fig. 3. π–A isotherm of the C_{60} film at 293 K.

calculated from the lattice parameters obtained from the ED pattern of Fig. 2(a) was 0.87 nm^2 $molecule^{-1}$. Therefore, it can be considered from the molecular occupied areas based on the π–A isotherm and ED pattern that the C_{60} molecules form a monolayer with macroscopic voids on the water subphase, even in the case of the dilute solution of 1.0×10^{-5} mol L^{-1}. Figure 4 shows the AFM images of the C_{60} films at the surface pressures of 10, 15, and 20 mN m^{-1} during the continuous compression process. The brighter parts in AFM image correspond to the higher height regions. The AFM

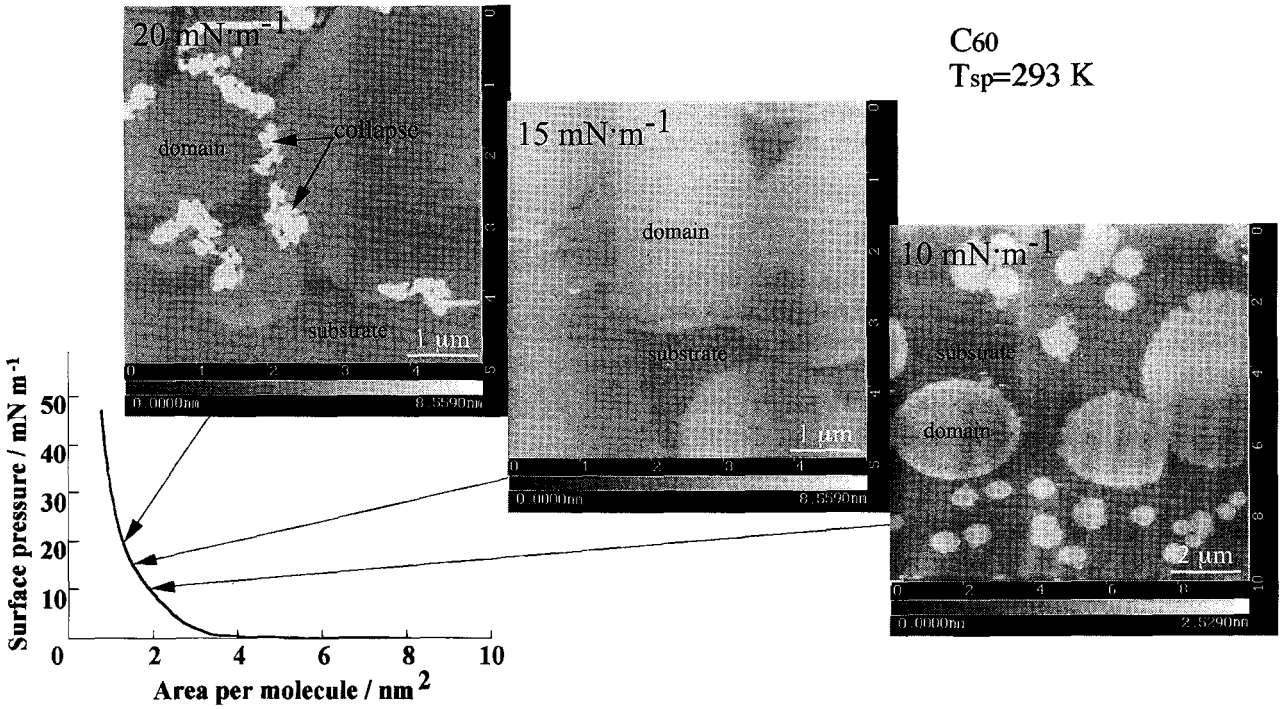

Fig. 4. AFM images of C_{60} films at surface pressures of 10, 15 and 20 mN m^{-1} in a process of continuous compression.

image of the C_{60} film directly compressed up to 20 mN m^{-1} taken at a certain region was fairly homogeneous, while that taken at another region was inhomogeneous as shown in Fig. 4. The AFM image of the C_{60} film at π of 20 mN m^{-1} in Fig. 4 was typical, which might indicate clearly the aggregation mechanism of the C_{60} film. The voids were observed as the spaces among the 2-dimensional C_{60} domains at the surface pressures of 10 and 15 mN m^{-1}. On the other hand, the 2-dimensional domains were collapsed in the domain boundary region in the case of the continuous compression up to the surface pressure of 20 mN m^{-1}, as shown in Fig. 4. The heights of the collapsed aggregates were higher than for the 2-dimensional C_{60} film. Therefore, it seems reasonable to conclude from Fig. 4 that there was not enough time to rearrange molecules in the C_{60} monolayer, induced by the structural relaxation at the domain boundaries in the case of the continuous compression up to the high surface pressure of 20 mN m^{-1}. Since the π–A isotherm in Fig. 3 showed no clear plateau region corresponding to the phase transition, it seems likely that the C_{60} film gradually collapsed at the domain boundaries by the continuous compression to a high surface pressure above 20 mN m^{-1} and then changed into the 3-dimensional one. Then Fig. 4 indicates that the continuous compression to the surface pressure of 20 mN m^{-1} is not appropriate to prepare the highly structure-regularized C_{60} monolayer with large area. Therefore, the area–creep method was applied to construct the highly structure-regularized C_{60} monolayer, as discussed next.

Preparation of C_{60} Monolayer by Multi-Step Creep Method. Figure 5 shows the time dependence of molecular occupied area for the C_{60} film at various surface pressures at T_{sp} of 293 K. The gray line shown in Fig. 5 represents the ideal molecular occupied area of the 2-dimensional C_{60} single

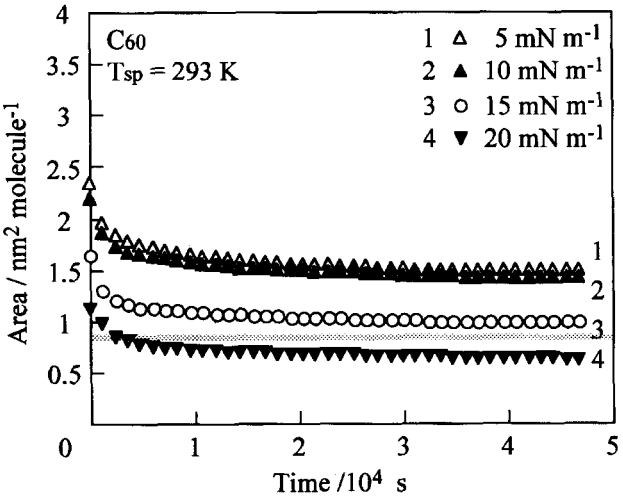

Fig. 5. Time dependence of molecular occupied area for the C_{60} film at the various surface pressures at T_{sp} of 293 K.

crystal packed in hexagonal array calculated from the lattice constants of the 3-dimensional C_{60} crystal.[32] The molecular occupied area of the C_{60} film at 20 mN m^{-1} was continuously decreased with the area–creep time studied in this experiment, perhaps due to the collapse of the film, as shown in the AFM image of Fig. 4. On the other hand, the molecular occupied area of the C_{60} film at surface pressures of 5, 10, and 15 mN m^{-1} became fairly constant after a long creep time. Similar area–creep behavior was observed for the stearic acid monolayer on the water surface and could be explained in terms of filling up the macroscopic and/or microscopic defects in the film without collapse.[24–26] Also, the molecular occupied area at the surface pressure of 15 mN m^{-1} after a long creep time became close to the calculated molecular

occupied area. Furthermore, the ED pattern of the C_{60} film prepared at the surface pressure of 15 mN m^{-1} after a long creep time was crystalline hexagonal spots. These results indicate that the area–creep at 15 mN m^{-1} at 293 K is useful for the construction of the highly structure-regularized C_{60} monolayer. However, the quasi-equilibrium molecular occupied area of the C_{60} film at the surface pressure of 15 mN m^{-1} after a long creep time was slightly larger than the molecular occupied area calculated for the C_{60} 2-dimensional single crystal. It is considered that this was due to the remaining vacancies which did not disappear due to the weak compression force of 15 mN m^{-1}. This indicates that further compression based on an area–creep, that is "multi-step creep method"[25] above 15 mN m^{-1} might be effective for the preparation of the highly regularized C_{60} monolayer.

Figure 6 shows the time dependence of molecular occupied area for the C_{60} film at various surface pressures during the successive multi-step creep processes. The gray line shown in Fig. 6 denotes the molecular occupied area calculated for the 2-dimensional C_{60} single crystal. The molecular occupied area of the C_{60} film became fairly constant with the area–creep time at each surface pressure. This may indicate that the structural relaxation at each surface pressure was almost completed. The molecular occupied area of the C_{60} film compressed up to 20 mN m^{-1} by the multi-step creep method agreed with the molecular occupied area of the 2-dimensional C_{60} crystal calculated based on the lattice constant of 3-dimensional C_{60} one. Then, the perfect 2-dimensional crystal of C_{60} could be prepared by the multi-step creep method on the water surface.

Figure 7 shows the AFM image of the C_{60} film prepared by the multi-step creep method up to π of 20 mN m^{-1}. The AFM image exhibited the fact that the C_{60} film was remarkably homogeneous, and no macroscopic defects or collapsed aggregation regions of the C_{60} film were observed. Also, after taking AFM image at a certain region, the AFM images at the other region were taken by moving the scanning area. In this manner, it was confirmed that the AFM images did not change over several hundred μm^2. In order to evaluate

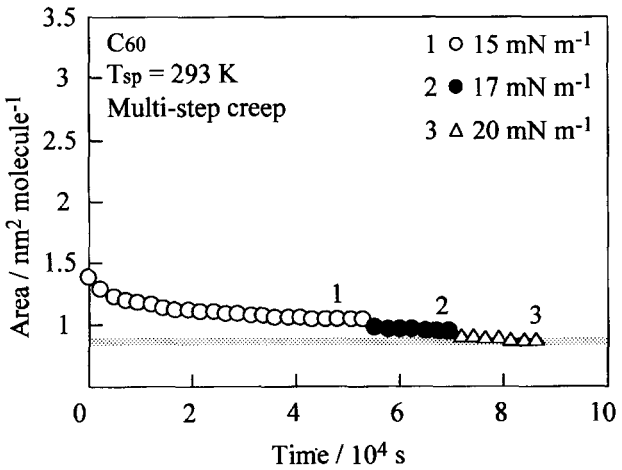

Fig. 6. Time dependence of molecular occupied area for the C_{60} film during the multi-step creep procedure.

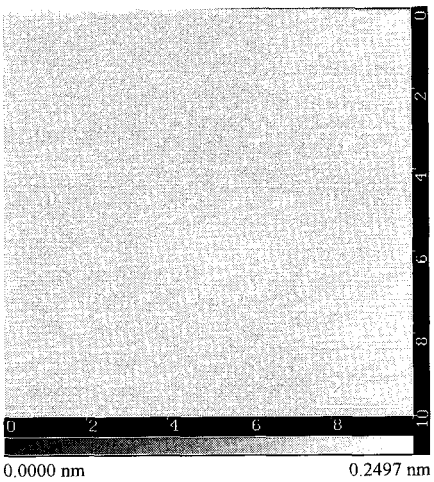

Fig. 7. AFM image of the C_{60} film at 20 mN m^{-1} prepared by the multi-step creep method.

the thickness of the C_{60} film prepared by the multi-step creep method, a pit was created in the C_{60} film by the AFM cantilever tip and the depth of the pit was measured by AFM observations. Figure 8 shows the AFM image of the pit created by the AFM cantilever tip in the C_{60} film prepared by the multi-step creep method and the height profile along the straight line shown in AFM image. The pit was made to the substrate by scratching the film repetitiously under the condition of increasing the applied force (ca. 10^{-8} N) of the AFM cantilever. Since the pit depth corresponds to the film thickness, Fig. 8 shows that the film thickness of the C_{60} film prepared by the multi-step creep method agreed well with the diameter of C_{60} molecule with π electron cloud. Therefore, it is reasonable to conclude that the C_{60} film prepared by the multi-step creep method was definitely composed of the monolayer.

Figure 9 shows the ED pattern of the C_{60} monolayer prepared by the multi-step creep method. The six sharp spots correspond to the (10) diffraction in the hexagonal array. The ED pattern of crystalline hexagonal spots for the C_{60} monolayer prepared by the multi-step creep method was much sharper along the azimuthal direction in comparison with the crystalline Debye ring for the C_{60} film prepared by the continuous compression, as shown in Fig. 2(b). It can be concluded from the comparison between Figs. 9 and 2(b) that C_{60} molecules in the C_{60} monolayer prepared by the multi-step creep method were regularly packed in the closely-packed hexagonal array with a high structural regularity, even if the C_{60} film was prepared at the higher surface pressure of 20 mN m^{-1}; compared with that, the C_{60} film prepared by the continuous compression was easily collapsed at this surface pressure.

Figure 10(a) shows the typical high-resolution AFM image in the area of 10×10 nm^2 of the C_{60} monolayer prepared by the multi-step creep method. Figure 10(b) shows the schematic representation for the AFM image corresponding to a magnification (5×5 nm^2) of the marked zone into Fig. 10(a). The white circles in Fig. 10(b) exhibit the protruded regions in the AFM image. Fig. 10(b) clearly indicates

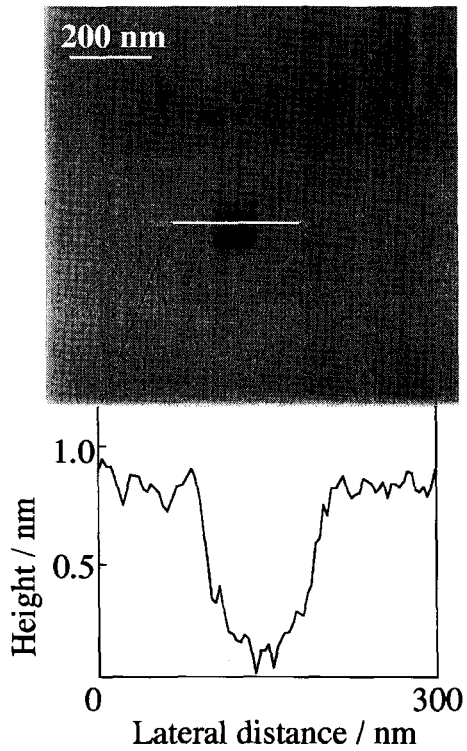

Fig. 8. AFM image of a pit created by the AFM cantilever in the C_{60} film prepared by the multi-step creep method and the height profile of the straight line into AFM image.

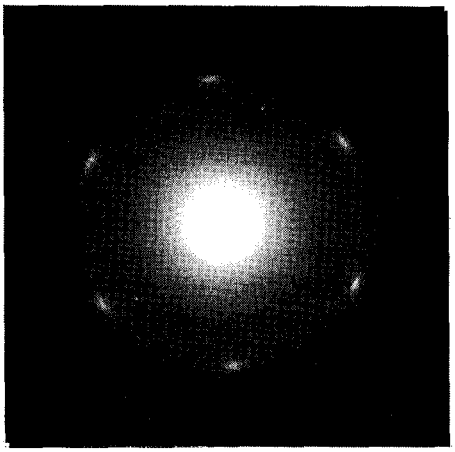

Fig. 9. ED pattern of the C_{60} monolayer prepared by the multi-step creep method.

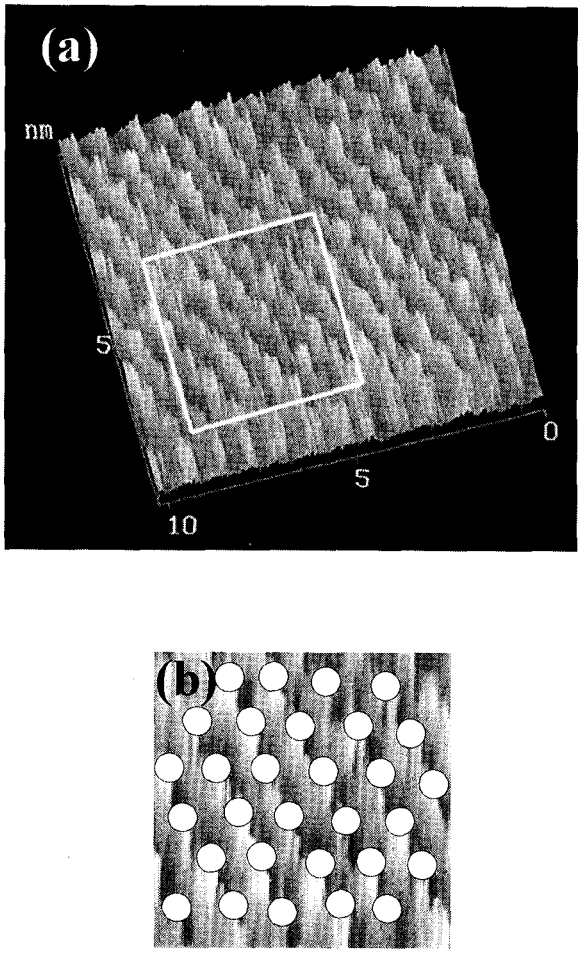

Fig. 10. High-resolution AFM image of the C_{60} monolayer at 20 mN m^{-1} prepared by the multi-step creep method. (a) High-resolution AFM image in the scan area of 10×10 nm^2. (b) Schematic representation for the AFM image corresponds to a magnification (5×5 nm^2) of the marked zone into Fig. 10(a). The white circles in Fig. 10(b) exhibit the protruded regions in the AFM image.

Table 1. Crystallographical Regularities of C_{60} Films Prepared by Continuous Compression and Multi-Step Creep Method

Methods	Crystallographical continuity, L_{lat}/nm	Crystallographical distortion, D_{lat}/%
Continuous compression	6.3	4.8
Multi-step creep	14.9	3.2

that these protruded regions regularly arranged into 2-dimensional hexagonal array. The (10) spacing evaluated from the AFM image was in good agreement with that evaluated from the ED pattern, as shown in Fig. 9. Therefore, we conclude that the highly projected points in Fig. 10 correspond to individual C_{60} molecules.

Table 1 summarizes the crystallographical regularities of the C_{60} films, that is, the magnitudes of the crystallographical distortion (D_{lat}) and the crystallographical continuity (L_{lat}). They were evaluated from the (10) ED profiles of the C_{60} films prepared by the continuous compression and the multi-step creep methods, respectively. The crystallographical regularity of the films in a lateral direction, that is, along the (10) directions was remarkably improved by structural relaxation during the step-wise area–creeps shown in Fig. 6. Since the 2-dimensional crystalline domains were gathered together by the continuous compression up to a high surface pressure directly in the case of the continuous compression method, it can be considered that there might be not enough time to carry out sufficient structural relaxation for filling up vacancies among the domains in the film, and also to rearrange the molecular packing in the film. The monolayer domains

may be easily collapsed due to stress concentration at the structural defects or vacancies which are mainly formed at the interfacial regions among the monolayer domains during the continuous compression, as shown in Fig. 4. On the other hand, in the case of the multi-step creep method, there might be sufficient time for the structural relaxation and molecular rearrangement during the step-wise area–creeps from a low surface pressure to a high surface pressure. Therefore, we conclude that the lateral crystallographical regularity of the monolayer prepared by the multi-step creep method was remarkably improved compared with the C_{60} film prepared by a conventional continuous compression method.

Conclusion. The multi-step creep method can provide the defect-diminished C_{60} monolayer by control of the structural relaxation induced by the area–creep. The C_{60} monolayer prepared by the multi-step creep has a homogeneous surface morphology and a high structural regularity, compared with these of the C_{60} film prepared by the conventional continuous compression method. Therefore, the multi-step creep method is quite effective for the construction of the defect-diminished C_{60} monolayer.

This work was in part supported by Grant-in-Aid for COE Research "Design and Control of Advanced Molecular Assembly Systems" (No. 08CE2005) from the Ministry of Education, Science, Sports and Culture. The authors thank T. Kuri (Kyushu University) and Dr. K. Tanaka (Kyushu University) for helpful discussions.

References

1 H. W. Kroto, J. R. Heath, S. C. O'Brien, R. F. Curl, and R. E. Smalley, *Nature*, **318**, 162 (1985).

2 W. Krätschmer, L. D. Lamb, K. Fostiropoulos, and D. R. Huffman, *Nature*, **347**, 354 (1990).

3 A. F. Hebard, M. J. Rosseinsky, R. C. Haddron, D. W. Murphy, S. H. Glarum, T. T. M. Palstra, A. P. Ramirez, and A. R. Kortan, *Nature*, **350**, 600 (1991).

4 P. W. Stephens, L. Mihaly, P. L. Lee, R. L. Whetten, S.-M. Hang, R. Kaner, F. Deiderich, and K. Holczer, *Nature*, **351**, 632 (1991).

5 K. Tanigaki, T. W. Ebbesen, S. Saito, J. Mizuki, J. S. Tsai, Y. Kudo, and S. Kuroshima, *Nature*, **352**, 222 (1991).

6 P. Wang, Y. Maruyama, and R. M. Metzger, *Langmuir*, **12**, 3932 (1996).

7 For example: S. Kazaoui, R. Ross, and N. Minami, *Solid State Commun.*, **90**, 623 (1994).

8 For example: a) H. Hoshi, N. Nakamura, Y. Maruyama, T. Nakagawa, S. Suzuki, H. Shiromaru, and Y. Achiba, *Jpn. J. Appl. Phys.*, **30**, L1397, (1991). b) Z. H. Kafafi, J. R. Lindle, R. G. Pong, F. J. Bartoli, L. J. Lingg, and J. Millile, *Chem. Phys. Lett.*, **188**, 492 (1992).

9 A. Ulman, "An Introduction to Ultrathin Organic Films: from Langmuir–Blodgett to Self-Assembly," Academic Press, Boston (1991).

10 Y. S. Obeng and A. J. Bard, *J. Am. Chem. Soc.*, **113**, 6279 (1991).

11 R. Back and R. B. Lennox, *J. Phys. Chem.*, **96**, 8149 (1992).

12 T. Nakamura, H. Tachibana, M. Yumura, M. Matsumoto, R. Azumi, M. Tanaka, and Y. Kawabata, *Langmuir*, **8**, 4 (1992).

13 M. Iwahashi, K. Kikushi, Y. Achiba, I. Ikemoto, T. Araki, T. Mochida, S. Yokoi, A. Tanaka, and K. Iriyama, *Langmuir*, **8**, 2980 (1992).

14 N. C. Maliszewskyj, P. A. Heiney, D. R. Jones, R. M. Strongin, M. A. Cichy, and A. B. Smith, *Langmuir*, **9**, 1439 (1993).

15 S. Uemura, A. Ohira, T. Ishizaki, M. Sakata, M. Kunitake, I. Taniguchi, and C. Hirayama, *Chem. Lett.*, **1999**, 279.

16 M. Matsumoto, H. Tachibana, R. Azumi, M. Tanaka, T. Nakamura, G. Yunome, M. Abe, S. Yamago, and E. Nakamura, *Lamgumir*, **11**, 660 (1995).

17 D. Vaknin, J. Y. Wang, and R. A. Uphaus, *Lamgmuir*, **11**, 1435 (1995).

18 D. A. Leigh, A. E. Moody, F. A. Wade, T. A. King, D. West, and G. S. Bahra, *Langmuir*, **11**, 2334 (1995).

19 S. Wang, R. M. Leblanc, F. Arias, and L. Echegoyen, *Langmuir*, **13**, 1672 (1997).

20 T. Kawai, S. Scheib, M. P. Cava, and R. M. Metzger, *Langmuir*, **13**, 5627 (1997).

21 Y. Xiao, Z. Yao, D. Jin, F. Yan, and Q. Xue, *J. Phys. Chem.*, **97**, 7072 (1993).

22 R. Rella, P. Siciliano, and L. Valli, *Thin Solid Films*, **243**, 367 (1994).

23 T. S. Berzina, V. I. Troitsky, O. Ya. Neilands, I. V. Sudmale, and C. Nicolini, *Thin Solid Films*, **256**, 186 (1995).

24 T. Kuri, Y. Oishi, and T. Kajiyama, *Bull. Chem. Soc. Jpn.*, **67**, 942 (1993).

25 T. Kuri, F. Hirose, Y. Oishi, K. Suehiro, and T. Kajiyama, *Langmuir*, **13**, 6497 (1997).

26 M. Yanagida, A. Takahara, and T. Kajiyama, *Bull. Chem. Soc. Jpn.*, **72**, 2795 (1999).

27 D. Volhardt, U. Retter, and S. Siegel, *Thin Solid Films*, **199**, 189 (1991).

28 R. Aveyard, B. P. Binks, N. Carr, A. W. Cross, G. W. Gray, and P. V. A. Kilvert, *Colloids Surf.*, **65**, 29 (1992).

29 M. Yanagida, T. Kuri, and T. Kajiyama, *Chem. Lett*, **1997**, 911.

30 Y. Oishi, T. Kuri, Y. Takashima, and T. Kajiyama, *Chem. Lett.*, **1994**, 1445.

31 D. Hofmann and E. Walenta, *Polymer*, **28**, 1271 (1987).

32 Diameter of C_{60} molecule was calculated from STM image (a) and molecular simulation (b); (a) for example: J. L. Wragg, J. E. Chamberlain, H. W. White, W. Krätschmer, and D. R. Huffman, *Nature*, **348**, 623 (1990). (b) S. Saito and A. Oshiyama, *Phys. Rev. Lett.*, **66**, 2637 (1991).

33 P. A. Heiney, J. E. Fischer, A. R. McGhie, W. J. Romanow, A. M. Denenstein, J. P. McCauley, Jr., and A. B. Smith, III, *Phys. Rev. Lett.*, **66**, 2911 (1991).